

# Diamonds and PAHs in the Circumstellar Environment of the Herbig Ae/Be Star Elias 1

R. Topalovic<sup>1</sup>, J. Russell<sup>1</sup>, J. McCombie<sup>1</sup>, T.H. Kerr<sup>2</sup> and P. J. Sarre<sup>1</sup>

<sup>1</sup>*School of Chemistry, The University of Nottingham, University Park, Nottingham NG7 2RD, U.K.*

<sup>2</sup>*United Kingdom Infrared Telescope, Joint Astronomy Centre, 660 N. A'ohoku Place, University Park, Hilo, Hawaii 96720, U.S.A.*

31 August 2018

## ABSTRACT

We report long-slit spectroscopic observations of the Herbig Ae/Be star Elias 1 in the 3.2 - 3.6  $\mu\text{m}$  region covering the C-H stretch emission features of hydrogen-terminated diamonds and PAHs. The data were recorded at UKIRT using UIST and yield information on the profiles and intensities of the bands as a function of offset along the N-S and E-W axes centred on the close binary. The diamond and nearby IR continuum emission arises from a symmetrical inner core region ( $\leq 0.34''$  or 48 AU). The 3.3  $\mu\text{m}$  PAH emission is extended along the E-W axis up to *c.* 100 AU each side of the star. This result supports a suggestion of Haas, Leinert & Richichi (1997) of an E-W oriented bipolar nebula in Elias 1.

**Key words:** stars: circumstellar matter –stars: binaries –stars: individual: V892 Tau

## 1 INTRODUCTION

The morphology, evolution and chemical composition of circumstellar disks and halos of pre-main-sequence intermediate-mass Herbig Ae/Be stars is of key importance in the study of star and planet formation (Waters & Waelkens 1998). Emission features of silicates and PAHs are commonly though not always observed (Acke & van den Ancker 2004) and in a few cases emission from surface-hydrogen-terminated diamonds is also detected. This raises interesting and challenging questions as to how the diamonds form, why their emission is seen in only a few stars, and whether there is a link between circumstellar diamonds and the presence of nanodiamonds in meteorites. The existence of organic PAHs in the nebular environment also provides astrobiological interest. In this paper we describe near-IR long-slit observations of one of the rare diamond C-H emitting objects, Elias 1. We focus on the spectroscopy and spatial distribution of diamond (C-H), PAH and continuum emission from the circumstellar environment, and make comparison with the related object HD 97048.

The pre-main-sequence star Elias 1 (V892 Tau, Elias 3-1) is a close binary with a separation of  $\sim 50$  mas at PA  $\sim 50^\circ$  (Smith et al. 2005). Its spectral type is uncertain ranging through A0 (Elias 1978), A6 with  $A_V = 3.9$  mag (Zinnecker & Preibisch 1994), B9 with  $A_V = 8.85$  mag (Strom & Strom 1994), with an  $A_V$  value of 10.5 also reported (Teixeira & Emerson 1999). Elias 1 has a very flat, possibly rising, SED in the near-IR to far-IR which is markedly different from that of HD 97048 (Hillenbrand et al.

1992), the two stars being classified as group II and I, respectively. The SED for Elias 1 is taken by Smith et al. (2005) to suggest the possible existence of an envelope in addition to a disk, or a flared disk. Other Elias 1 characteristics include X-ray (Zinnecker & Preibisch 1994; Giardino et al. 2004; Hamaguchi, Yamauchi & Koyama 2005; Stelzer et al. 2006) and radio (Skinner, Brown & Stewart 1993) emission.

An emission feature in the *c.* 3.5  $\mu\text{m}$  region for Elias 1 was first reported in 1982 by Allen et al. (1982) and was subsequently shown to have two components near 3.41 and 3.52  $\mu\text{m}$  with an additional PAH feature at 3.29  $\mu\text{m}$  (Whittet et al. 1983). The only previously detected example was HD 97048 (Blades & Whittet 1980). Subsequent spectroscopic observations of Elias 1 have been made (Whittet, McFazdean & Geballe 1984; Tokunaga et al. 1991; Geballe 1997), including ISO (SWS) data (Van Kerckhoven, Tielens & Waelkens 2002). The features at 3.43 and 3.53  $\mu\text{m}$  remained unassigned until Guillois, Ledoux & Reynaud (1999) found a convincing correspondence between the astrophysical bands of Elias 1 and HD 97048 and laboratory absorption spectra of the C-H stretching modes on hydrogen-terminated diamond nanocrystal films at  $\sim 1000$  K (Chang et al. 1995). ISO spectra of Elias 1 covering the range 2.5 - 13.5  $\mu\text{m}$  (Van Kerckhoven, Tielens & Waelkens 2002) contain absorption features due to water and CO<sub>2</sub> ice, and emission from PAHs, diamonds and silicates, the last of these being absent from the spectrum of HD 97048. In this paper we have chosen not to use the word ‘nanodiamond’ in discussing the stellar emission features as their size is probably at least 50 nm (Chen et al. 2002; Sheu et al. 2002; Jones et al.

2004) in contrast to meteoritic nanodiamonds which are typically only 2-3 nm across (Lewis et al. 1987). We also remark that the diamonds observed are exclusively those that are H-terminated at the surface; absence of hydrogen or its substitution by other chemical groups on the surface in general give spectra outside the region studied. The only other Herbig Ae/Be objects for which diamond emission is reported are BD+40°4124 (Acke & van den Ancker 2004) and MWC 297 (Terada et al. 2001; Acke & van den Ancker 2004); emission features attributed to diamond emission are also seen in the post-AGB star HR 4049 (Geballe et al. 1989) but are relatively weak.

## 2 THE CIRCUMSTELLAR ENVIRONMENT OF ELIAS 1

Unresolved at mm wavelengths (di Francesco et al. 1997; Henning et al. 1998), observations of the spatial distribution of the circumstellar emission of Elias 1 comprise a contour map of the inner  $0.2'' \times 0.2''$  region which exhibits asymmetry along the binary PA of  $50^\circ$  (Smith et al. 2005), and speckle interferograms at K, L ( $0^\circ$  and  $90^\circ$ ) and L' at  $45^\circ$  (Kataza & Maihara 1991) and at J, H, K and L' (Haas, Leinert & Richichi 1997). Kataza & Maihara (1991) interpreted their data in terms of a core with a wavelength-dependent diameter of  $\sim 6$ -14 AU, and a highly flattened halo elongated in the east-west direction with radius  $\sim 30$ -100 AU in the form of a nearly edge-on circumstellar disk. Based on observations covering a wider range of wavelengths and at higher resolution, Haas, Leinert & Richichi (1997) proposed that the east-west elongation is due to scattered light from bipolar (nebular) lobes. From the PA  $90^\circ$  and  $0^\circ$  data it was concluded that the components observed at J and H comprise a well-resolved narrow blue structure elongated east-west with a FWHM of  $c. 1''$  and a second that is marginally resolved (FWHM  $\leq 0.2''$ ), and that there is marginally resolved red structure at K and L' which is more circular and symmetric. From a consideration of all the available data and a number of possible interpretations, Haas, Leinert & Richichi (1997) proposed the existence of a bipolar nebula along the E-W axis as the origin of the E-W extension. They also discussed the existence of a possible stellar companion, noting that their K and L' data could be fitted by a close binary with separation oriented at PA  $45^\circ$  or  $135^\circ$  with separation  $< 0.1''$ , together with some extended structure. Recent diffraction-limited speckle interferometric observations confirm that Elias 1 is indeed a close binary system with these characteristics, the separation being  $0.05''$  with PA  $50^\circ$  (Smith et al. 2005).

## 3 OBSERVATIONS

Observations of the Herbig Ae/Be star Elias 1 were carried out between 20th July - 11th September 2004 at the 3.8 m United Kingdom Infrared Telescope (UKIRT). The 1 - 5  $\mu\text{m}$  imager-spectrometer (UIST) was used for the long-slit spectroscopic observations. The slit dimensions were  $0.48'' \times 120''$  and the resolving power = 700. The short-L grism was used to obtain spectra in the wavelength region 2.905 -

**Table 1.** Observing log

	Date (2004)	slit	exp (sec)	standard	PSF FWHM( $''$ )
Elias 1	Jul 20	N-S	80	BS 1203	0.53
Elias 1	Jul 28	N-S	128	BS 1203	0.52
Elias 1	Sep 11	N-S	80	BS 1203	0.55
Elias 1	Sep 11	E-W	80	BS 1203	0.52

3.638  $\mu\text{m}$  in combination with an InSb array of  $1024 \times 1024$  pixels, giving a spatial resolution of  $0.12'' \text{ pix}^{-1}$ . The slit was centred on the star and orientated at position angles  $0^\circ$  (NS) and  $90^\circ$  (WE). The observational details are listed in table 1. The sky background emission was subtracted from the standard and object frames and the object spectra were divided by the standard. The point spread function (PSF) of the observations is very consistent. A further exposure along E-W was made on 27 July but due to poor seeing the PSF was  $c. 0.7''$  and was not included in this analysis.

The data were partially reduced by the ORAC-DR (automated reduction) pipeline for UIST and further reductions were carried out with the FIGARO reduction package. The spectra were analysed using the IRAF reduction package; the continuum was fitted and subtracted from the spectra and Lorentzians were used to fit the emission bands.

## 4 INFRARED SPECTROSCOPIC FEATURES AND SPATIAL DISTRIBUTIONS

### 4.1 H-terminated diamond and PAH spectra

In common with similar long-slit studies of Red Rectangle PAH features (Song et al. 2003), one of the objectives was to investigate any evolution in profile shape, central wavelength etc. of the PAH C-H stretch and (particularly) the C-H diamond features with increase in offset from the star. The summed 3.0 - 3.6  $\mu\text{m}$  spectra for Elias 1 along the N-S axis for the inner  $\pm 0.3''$  relative to the star are shown in Fig 1 and are similar to the UKIRT data of (Geballe 1997) although the Pf $\delta$  line of hydrogen which sits atop the 3.3  $\mu\text{m}$  PAH band is much weaker in our spectra. The Pf $\delta$  flux in our 2004 data is  $c. 0.2 \times 10^{-13} \text{ Wm}^{-2} \mu\text{m}^{-1}$  compared with  $c. 1.0 \times 10^{-13} \text{ Wm}^{-2} \mu\text{m}^{-1}$  (Geballe 1997). The assignments of the C-H diamond features have been described elsewhere (Guillois, Ledoux & Reynaud 1999; Van Kerckhoven, Tielens & Waelkens 2002) and are not reproduced here. The best match between experimental absorption spectra and the astrophysical data is achieved for a temperature of  $c. 1000 \text{ K}$  (Guillois, Ledoux & Reynaud 1999; Van Kerckhoven, Tielens & Waelkens 2002). Laboratory data have revealed a strong dependence of the spectrum on particle size, indicating that the diamonds in Elias 1 (and HD 97048) are probably at least 50 nm in diameter and are likely formed in a CVD-type process (Chen et al. 2002; Sheu et al. 2002; Jones et al. 2004).

As described in the following sub-section, the diamond distribution in Elias 1 is confined to a region quite close to the star within  $\leq 48 \text{ AU}$  (FWHM, Gaussian fitted). By taking data extractions 'on-star' at the point of maximum emission strength and secondly at the greatest possible off-

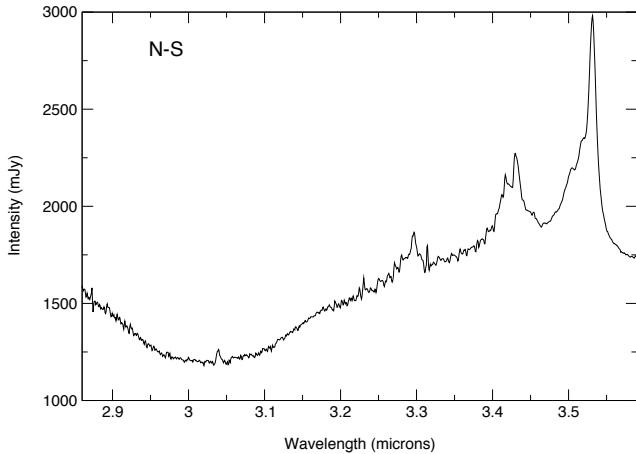


**Figure 1.** Co-added spectra of Elias 1 in the 2.9 - 3.6  $\mu\text{m}$  region recorded with slit alignment N-S. The data were summed over the inner  $\pm 0.3''$ . The data for E-W are the same within the signal-to-noise ratio.

set for which a reasonable signal-to-noise is still maintained, we searched for variation in the diamond features but did not find evidence for this to within 0.15% (in  $\lambda$ ), 20% (in FWHM), and 10% (in relative intensity). The PSF of *c.*  $0.5''$  is larger than desirable relative to the diamond emission spatial extent of  $\text{FWHM} \leq 0.34''$ . However, changes in the relative band strengths of the components, in peak wavelength or in profile shape that might occur due to change in temperature with offset, diamond size effects on the spectra, or in the relative emission contributions of the different C-H supporting diamond facets, would be discernible. This result points to a rather specific set of formation conditions and/or surface chemistry, possibly not unrelated to the rarity of the appearance of the features.

Of the main PAH emission bands, only the relatively weak  $3.3\mu\text{m}$  feature occurs in the spectral range recorded and is subject to contamination by telluric methane and water lines, as well as from the Pf $\delta$  emission line of the star. As for the diamond emission bands there was no measurable change in the feature profile with offset but a 20% change in width would have been detected.

#### 4.2 Spatial distributions of PAH, diamond and continuum emission

Slit alignments along the N-S and the E-W axes were selected in order to probe the spatial distribution of the PAH ( $3.3\mu\text{m}$ ), diamond and continuum emission relative to the star. Although adaptive optics and larger mirror size (and speckle interferometric observations) offer a lower effective PSF, high signal-to-noise data achieved with moderate exposure times and at high altitude on Mauna Kea provide an attractive option with relatively straightforward data reduction procedures. Determination of the PSF was achieved using the standard (point source) star BS 1203 and gave a stable value of  $0.53(2)''$  (see table 1.)

The N-S and E-W spatial distributions as recorded for the PAH ( $3.3\mu\text{m}$ , continuum-subtracted), diamond ( $3.53\mu\text{m}$ , continuum-subtracted) and continuum ( $3.60\mu\text{m}$ ) are given in figs 2 and 3, respectively. The set of diamond

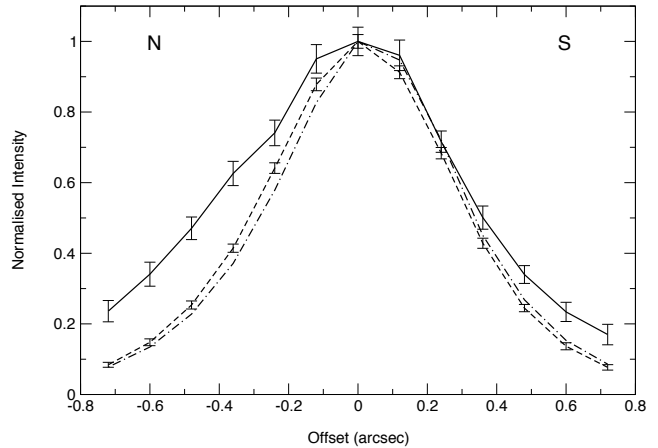


**Figure 2.** Normalised emission intensities along the N-S axis for the PAH ( $3.3\mu\text{m}$ ) - solid line, diamond ( $3.53\mu\text{m}$ ) - dashed line, and continuum ( $3.60\mu\text{m}$ ) - dot-dashed line.

features near  $3.43\mu\text{m}$  follow the  $3.53\mu\text{m}$  distribution within signal-to-noise constraints, the measured spatial FWHM for  $3.53\mu\text{m}$  being  $0.590''$  (NS) and  $0.603''$  (EW), and  $0.603''$  (NS) and  $0.597''$  (EW) for the  $3.43\mu\text{m}$  group. Figs 4 and 5 show the results when a Richardson-Lucy (RL) deconvolution algorithm was employed to deconvolve the profiles. For the N-S slit position ( $\text{PA} = 0^\circ$ ) in fig 4 the profiles for PAH, diamond and continuum overlap very well for the inner  $\pm 0.2''$ , with the latter two overlapping for all offsets. However, the PAH distribution extends weakly about three times further, with slightly greater strength in the N direction. For the E-W slit position ( $\text{PA} = 90^\circ$ ) shown in figure 5 the diamond and continuum distributions are the same within the signal-to-noise. In contrast, the PAH distribution is very broad and skewed slightly towards W.

The deconvolved continuum-subtracted  $3.53\mu\text{m}$  Elias 1 diamond feature shows a symmetrical distribution N, S, E and W of the central star. This is consistent with the circular symmetric component described by Haas, Leinert & Richichi (1997) for K and L' who noted that the latter filter at  $3.69 \pm 0.315\mu\text{m}$  includes the strong  $3.42$  and  $3.53\mu\text{m}$  features observed in our study and that are now known to be due to diamond emission. The distribution for diamond emission has a FWHM of  $0.34''$  giving a Gaussian FWHM diameter of  $\leq 48$  AU where a distance to Elias 1 of 140 pc (Elias 1978) was adopted. The continuum profile that is generally taken to arise from thermal emission by larger grains is very similar.

The PAH distribution is extended relative to diamond and continuum emission along both slit axes but more so for E-W than N-S. For E-W a signal is discernible to  $\pm 0.7''$  or  $\pm 100$  AU W and E relative to the star. This long-slit spectroscopic result agrees well with the findings of Haas, Leinert & Richichi (1997) who found a narrow E-W elongated blue halo in J and H with FWHM of about  $1''$ , the N-S extent only being about  $0.2''$ . We conclude that the new data provide strong evidence for a PAH-containing bipolar nebula oriented close to E-W but, given the asymmetry in the PAH distribution along both E-W and N-S (see figs 4 and 5), tilted slightly with respect to the observer.

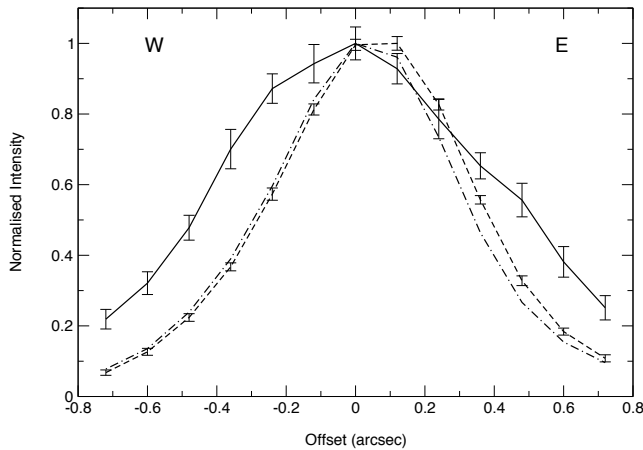


**Figure 3.** Normalised emission intensities along the E-W axis for the PAH ( $3.3 \mu\text{m}$ ) - solid line, diamond ( $3.53 \mu\text{m}$ ) - dashed line, and continuum ( $3.60 \mu\text{m}$ ) - dot-dashed line.

## 5 COMPARISON OF ELIAS 1 WITH HD 97048

It is of interest to compare the results for Elias 1 with those for HD 97048. There is a clear similarity in that they both exhibit PAH, diamond and IR continuum emission, but they have very different SEDs and fall in different classifications being in Group II with a large IR excess (Elias 1) and in Group I (HD 97048) with a circumstellar disk seen pole-on (Hillenbrand et al. 1992; Habart et al. 2004).

Based on speckle observations, Roche, Allen & Bailey (1986) reported that the  $3.53 \mu\text{m}$  diamond emission of HD 97048 is not substantially extended, arising within  $0.1''$  of the star. Habart et al. (2004) more recently described an adaptive optics high angular resolution (*c.*  $0.1''$ ) long-slit spectral study of the spatial distribution of diamond and continuum emission for HD 97048. It was deduced that the FWHM sizes are consistent with predictions for a circumstellar disk oriented pole-on, with the diamond emission originating in an inner region. The diamond FWHM emission for HD 97048 is reported by Habart et al. (2006) to be 41 AU and that of the continuum 32 AU, which compare with our Elias 1 results of  $\leq 0.34''$  (48 AU) for both diamond and the continuum.

Habart et al. (2006) have reported spatially resolved  $3.3 \mu\text{m}$  PAH emission for HD 97048 which is more extended than the diamond and continuum emission and hence similar to our results for Elias 1. The PAH distribution data for HD 97048 is incomplete due to a noisy section near  $3.3 \mu\text{m}$  falling in the  $+0.0 - 0.2''$  region and a value for the FWHM was not quoted. However, from the negative offset data (figure 3 of the paper) and assuming a symmetrical spatial profile, a FWHM of  $\sim 60$  AU can be estimated. An extended  $3.3 \mu\text{m}$  distribution for HD 97048 is also consistent with a comparison between the ISO-SWS ( $20'' \times 33''$ ) spectrum and the spectra of Habart et al. (2004) within  $1''$  of the star which showed the PAH  $3.3 \mu\text{m}$  band to be stronger relative to the diamond bands in the ISO spectrum. Resolved PAH profiles in other Herbig Ae/Be stars have been found and successfully modelled by Habart, Natta & Krügel (2004). In general the  $3.3 \mu\text{m}$  PAH feature tends to be more confined spatially than the UIR bands at  $6.2$ ,  $7.7$ ,  $8.6$  and  $11.2 \mu\text{m}$ . This is so for HD 97048 which extends *c.*  $5 - 10''$  in the

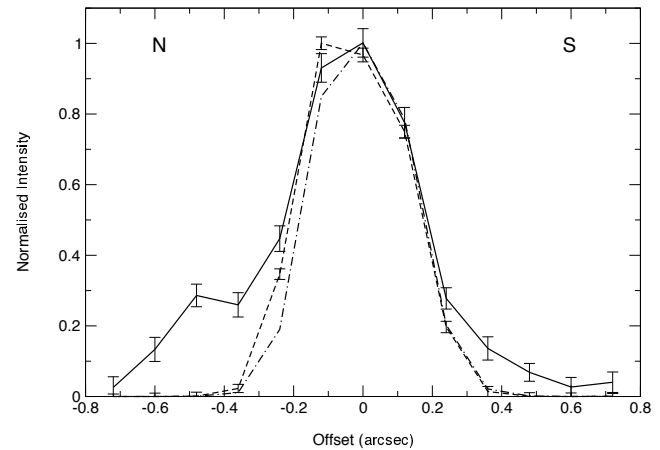


**Figure 4.** Normalised emission intensities along the N-S axis for the PAH ( $3.3 \mu\text{m}$ ) - solid line, diamond ( $3.53 \mu\text{m}$ ) - dashed line, and continuum ( $3.60 \mu\text{m}$ ) - dot-dashed line, where the data for different nights (see table 1.) are co-added and a RL deconvolution applied.

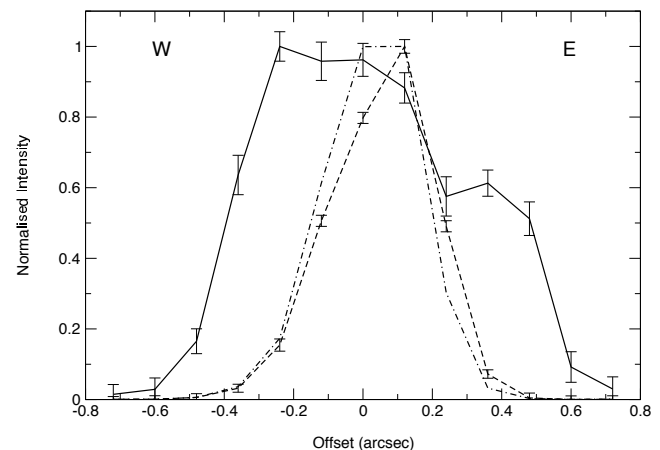


**Figure 5.** Normalised emission intensities along the E-W axis for the PAH ( $3.3 \mu\text{m}$ ) - solid line, diamond ( $3.53 \mu\text{m}$ ) - dashed line, and continuum ( $3.60 \mu\text{m}$ ) - dot-dashed line, where a RL deconvolution has been applied.

mid-IR (Siebenmorgen et al. 2000) and from limited nulling interferometric observations is reported to be the case for Elias 1 (Liu et al. 2005).

## 6 SUMMARY

We have conducted a long-slit study of Elias 1 in the  $3.2 - 3.6 \mu\text{m}$  region which has revealed a symmetrical distribution for the continuum ( $3.6 \mu\text{m}$ ) and diamond C-H emission features, and more extended PAH  $3.3 \mu\text{m}$  emission which is oriented along the E-W axis. Given that for many objects the  $3.3 \mu\text{m}$  PAH emission is significantly less extended than for the UIR bands at longer wavelengths, it will be of interest to determine the mid-IR PAH emission distribution using long-slit spectroscopy in order to probe the size and geometry of the bipolar nebula.

## 7 ACKNOWLEDGMENTS

We thank the UK Panel for the Allocation of Telescope Time for the award of observing time on UKIRT, PPARC for a studentship to RT and EPSRC for a studentship to JR.

## REFERENCES

- Acke, B., van den Ancker, M.E., 2004, *A&A*, 426, 151  
 Allen, D.A., Baines, D.W.T., Blades, J.C., Whittet, D.C.B., 1982, *MNRAS*, 199, 1017  
 Blades, J.C., Whittet, D.C.B., 1980, *MNRAS*, 191, 701  
 Chang, H.-C., Lin, J.C., Wu, J.Y., Chen, K.-H., 1995, *J. Phys. Chem.*, 99, 11081  
 Chen, C.-F., Wu, C.-C., Cheng, C.-L., Sheu, S.-Y., Chang, H.-C., 2002, *JChPh*, 116, 1211  
 di Francesco, J., Evans, N.J., Harvey, P.M., Mundy, L.G., Guilloteau, S., Chandler, C.J., 1997, *ApJ*, 482, 433  
 Elias, J.H., 1978, *ApJ*, 224, 857  
 Geballe, T.R., Noll, K.S., Whittet, D.C.B., Waters, L.B.F.M., 1989, *ApJ*, 340, L29  
 Geballe, T.R., 1997, in 'From Stardust to Planetesimals' Symposium, ASP Conference Series, 122, ed. Yvonne J. Pendleton, A.G.G.M. Tielens, p.119  
 Giardino, G., Favata, F., Micela, G., Reale, F., 2004, *A&A*, 413, 669  
 Guillois, O., Ledoux, G., Reynaud, C., 1999, *ApJ*, 521, L133  
 Haas, M., Leinert, C., Richichi, A., 1997, *A&A*, 326, 1076  
 Habart, L., Natta, A., Testi, L., Carbillet, M., 2004, *ApJ*, 614, L129  
 Habart, E., Natta, A., Krügel, E., 2004, *A&A*, 427, 179  
 Habart, E., Natta, A., Testi, L., Carbillet, M., 2006, *A&A*, 449, 1067  
 Hamaguchi, K., Yamauchi, S., Koyama, K., 2005, *ApJ*, 618, 360  
 Henning, Th., Burkert, A., Launhardt, R., Leinert, Ch., Stecklum, B., 1998, *A&A*, 336, 565  
 Hillenbrand, L.A., Strom, S.E., Vrba, F.J., Keene, J., 1992, *ApJ*, 397, 613  
 Jones, A.P., d'Hendecourt, L.B., Sheu, S.-Y., Chang, H.-C., Cheng, C.-L., Hill, H.G.M., 2004, *A&A*, 416, 235  
 Kataza, H., Maihara, T., 1991, *A&A*, 248, L1  
 Lewis, R.S., Ming, T., Wacker, J.F., Anders, E., Steel, E., 1987, *Nat*, 326, 160  
 Liu, W.M., Hinz, P.M., Hoffmann, W.F., Brusa, G., Miller, D., Kenworthy, M.A., 2005, *ApJ*, 618, L133  
 Roche, P.F., Allen, D.A., Bailey, J.A., 1986, *MNRAS*, 220, 7P  
 Sheu, S.-Y., Lee, I.-P., Lee, Y.T., Chang, H.-C., 2002, *ApJ*, 581, L55  
 Siebenmorgen, R., Prusti, T., Natta, A., Müller, T.G., 2000, *A&A*, 361, 258, and references therein.  
 Skinner, S.L., Brown, A., Stewart, R.T., 1993, *ApJS*, 87, 217  
 Smith, K.W., Balega, Y.Y., Duschl, W.J., Hofmann, K.-H., Lachaume, R., Preibisch, T., Schertl, D., Weigelt, G., 2005, *A&A*, 431, 307  
 Song, I.-O., Kerr, T.H., McCombie, J., Sarre, P.J., 2003, *MNRAS*, 346, L1  
 Stelzer, B., Micela, G., Hamaguchi, K., Schmitt, J.H.M.M., 2006, *A&A* (astro-ph/0605590)  
 Strom, K.M., Strom, S.E., 1994, *ApJ*, 424, 237  
 Teixeira, T.C., Emerson, J.P., 1999, *A&A*, 351, 303  
 Terada, H., Imanishi, M., Goto, M., Maihara, T., 2001, *A&A*, 377, 994  
 Tokunaga A.T., Sellgren K., Smith R.G., Nagata T., Sakata A., Nakada Y., 1991, *ApJ*, 380, 452  
 Van Kerckhoven, C., Tielens, A.G.G.M., Waelkens, C., (2002) *A&A*, 384, 568  
 Waters, L.B.F.M., Waelkens, C., 1998, *ARA&A*, 36, 233  
 Whittet, D.C.B., Williams, P.M., Zealey, W.J., Bode, M.F., Davies, J.K., 1983, *A&A*, 123, 301  
 Whittet, D.C.B., McFazdean, A.D., Geballe, T.R., 1984, *MNRAS*, 211, 29P  
 Zinnecker, H., Preibisch, Th., 1994, *A&A*, 292, 152